Accepted Manuscript

Structural and Magnetic behavior of ferrogels obtained by freezing thawing of polyvinyl alcohol/poly(acrylic acid) (paa)-coated iron oxide nanoparticles

O. Moscoso-Londoño, J.S. Gonzalez, D. Muraca, C.E. Hoppe, V.A. Alvarez, A. López-Quintela, L. M. Socolovsky, K. R. Pirota

Please cite this article as: Moscoso-Londoño, O., Gonzalez, J.S., Muraca, D., Hoppe, C.E., Alvarez, V.A., López-Quintela, A., M. Socolovsky, L., R. Pirota, K., Structural and Magnetic behavior of ferrogels obtained by freezing thawing of polyvinyl alcohol/poly(acrylic acid) (paa)-coated iron oxide nanoparticles, *European Polymer Journal* (2012), doi: http://dx.doi.org/10.1016/j.eurpolymj.2012.11.007

STRUCTURAL AND MAGNETIC BEHAVIOR OF FERROGELS OBTAINED BY FREEZING THAWING OF POLYVINYL ALCOHOL/POLY(ACRYLIC ACID) (PAA)-COATED IRON OXIDE NANOPARTICLES

O. Moscoso-Londoño[a], J.S. Gonzalez[b*], D. Muraca[c], C. E. Hoppe[b], V.A. Alvarez[b,], A. López-Quintela[d], L. M. Socolovsky[a], K. R. Pirota[c].

[a] *Laboratorio de Sólidos Amorfos (LSA), INTECIN, Facultad de Ingeniería*, Universidad de Buenos Aires - CONICET, C1063ACV, Buenos Aires, Argentina.

[b] *Institute of Materials Science and Technology (INTEMA),* University of Mar del Plata (UNMdP) and National Research Council (*CONICET*), Av. J. B. Justo 4302, (B7608FDQ) Mar del Plata, Argentina.

[c] *Laboratorio de Materiais e Baixas Temperaturas (LMBT),* Instituto de Física 'Gleb Wataghin', Universidade Estadual de Campinas, CEP 13083-859, Campinas-SP, Brazil

[d] *Departamento de Química Física, Facultad de Química*, Universidad de Santiago de Compostela (USC), 15782, Santiago de Compostela, España.

* Corresponding author: jimena.gonzalez@fi.mdp.edu.ar. Institute of Materials Science and Technology (INTEMA), University of Mar del Plata (UNMdP) and National Research Council (CONICET), Solís 7575 (B7608FLC) Mar del Plata, Argentina TE: +54 223 481 6600 ext. 321. FAX: +54 223 481 0046.

1

ABSTRACT

Superparamagnetic ferrogels with high swelling ability and potential applications as solvent absorbers and stimuli-responsive drug delivery devices were obtained by a non-toxic and environmentally friendly route based on dispersion of poly(acrylic acid)-coated iron oxide nanoparticles (PAA-coated NPs) in poly(vinyl alcohol) (PVA) solutions followed by freezing-thawing. Presence of carboxylate groups arising from the PAA coating allowed hydrogen bonding formation between NPs and PVA and enabled the synthesis of optically homogenous, superparamagnetic materials formed by a homogenous distribution of NPs diffuse clusters in the PVA matrix. The addition of PAA-coated NPs produced a remarkable increase in crystallinity degree, thermal degradation and swelling percentage respect to the neat matrix, which demonstrates that ferrogels with improved properties can be obtained by this procedure. Thereafter, combination of a cryogenic technique with the use of non-toxic components and magnetic NPs coated by a pH sensitive polymer makes these ferrogels very promising for applications in the biomedical field.

2

1. INTRODUCTION

Polymer gels are wet and soft materials constituted by networks of flexible cross-linked chains with a fluid filling their interstitial space [1]. They are fascinating materials with multiple and diverse applications as separator agents, solvent absorbers, ion exchangers, diapers, drug delivery devices, etc [2-5]. Although these examples show that products based on hydrogels (arising from many different natural or synthetic polymers) have had an enormous impact in the field of medicine and patient care, today, new and more sophisticated applications, as stem cell research, drug delivery, tissue engineering, in vitro diagnostics, among others, require more than good chemical and mechanical properties from these materials [6-8]. Tuning of network porosity, affinity to specific therapeutic drugs and bio-molecules, responsiveness of the porous structure to external stimuli, control on architectural features, etc. are some of the design challenges to face, in order to prepare materials with potential clinical applications. Furthermore, from an ideal point of view, these characteristics should be attained by the use of non-toxic, non-expensive and biocompatible reactants and processing techniques.

Formation of hydrogels can be carried out by diverse techniques like chemical crosslinking, photo-polymerization, gamma or electron irradiation and freezing-thawing (F-T), among others. F-T is a cryogenic technique that has been successfully used for the crosslinking of a number of polymers [1, 9-10]. Main advantages associated with the use of F-T can be found in the good physical and mechanical properties of the gels obtained, the simplicity of the technique, the use of low temperatures and the absence of any leachable toxic crosslinking agents or other waste that can be harmful to the human body [11].

Hydrogels can be used as matrices for the development of new advanced functional materials like ferrogels with new and interesting magnetic and mechanical properties [12-15]. Ferrogels play an important role in the development of new devices of fundamental interest in the biomedical and pharmaceutical fields like sensors, artificial muscles, drug delivery devices, etc.

[16-18]. They are obtained by dispersion of magnetic NPs in a soft gel matrix and constitute one relevant example of nanostructured magnetic systems.

To obtain a ferrogel, incorporation of magnetic NPs can be performed following diverse procedures [11]. Among them, dispersion of preformed magnetic NPs (of a specific size, shape and coating) in a polymer solution that could be subsequently crosslinked, results attractive as a strategy to obtain nanocomposites with well controlled and predictable properties. Non-toxicity and biocompatibility of magnetic iron oxide nanoparticles (NPs), like magnetite (Fe_3O_4) and maghemite ($\gamma\text{-}Fe_2O_3$), make them the natural choice for the synthesis of materials with potential biomedical applications [17, 19-20]. Most of these applications require ferrogels with high filler concentrations (close proximity among NPs) and, at the same time, a good level of dispersion of NPs in the matrix. This is important because it has been demonstrated that extensive aggregation can eliminate many of the advantages associated with the use of nanometric fillers, especially when individuality of NPs is not preserved or in presence of macroscopic aggregation. More important, distribution of magnetic NPs in the matrix strongly controls final magnetic properties of ferrogels. In concentrated systems, the influence of magnetic dipolar interactions between closest neighbours becomes significant, affecting the macroscopic magnetic properties of the material. For this reason is fundamental both, to design strategies that enable the control of the dispersion level of NPs in the matrix and to understand the role of NPs distribution, the effect of the formation of assemblies and aggregates, and the influence of possible interactions between magnetic NPs on the final behaviour of materials, after and during fabrication. The importance of these variables on the magnetic properties of real nanocomposites is reflected in the large number of studies that have been reported regarding the magnetic response of iron oxide NPs and magnetic ferrites entrapped in different kinds of polymers, or as ferrofluids, as a function of concentration [21-26].

By proper selection of NPs coating, affinity between NPs and matrix can be favored, leading to the improvement of the dispersion level of NPs in the matrix and to the formation of well

4

dispersed and robust ferrogel systems. Furthermore, NPs coating can add special functionalities and responsiveness to the final material, enhancing their potential applications.

PVA, a well-known biocompatible polymer with a good gel forming capability, is an ideal candidate for the synthesis of ferrogels and has been previously used as matrix to disperse metallic and magnetic NPs for diverse applications [27-34]. Poly(acrylic acid) (PAA) is a biocompatible, pH-responsive polyelectrolyte (pKa 4.5) that provokes little antigenic reaction *in vivo* [35]. Because of ionization of carboxylic acid groups, charge density of PAA chains is strongly dependent on pH. Hence, PAA is very sensitive to pH and ionic strength, which make it very useful for the design of polymer networks with stimuli-responsive load and release abilities [36-39]. In fact, acrylic acid has already been used for the synthesis of inter-penetrating networks (IPNs) and copolymers that exhibit thermo-, electro- and pH-responsive behavior [35, 37]. More recently, PAA proved to be useful for the synthesis of PAA-coated magnetic NPs with the ability to adsorb basic dyes and basic proteins [40], to enhance the mobility of magnetic NPs with potential applications in groundwater remediation applications [41], for the synthesis of controlled magnetic aggregates, [42] and for the synthesis of Janus NPs that can be reversibly self-assembled by controlling pH [43-44]. Thus, PAA could be an interesting choice as possible coating of magnetic NPs forming ferrogels.

The main objective of this work is to synthesize ferrogels by dispersion of functional, PAA-coated magnetic NPs in PVA aqueous solutions followed by physical crosslinking of the polymer chains by a F-T method. The general idea behind this work is that the presence of PAA in the surface of NPs could facilitate the formation of strong hydrogen-bond interactions between NPs and the PVA matrix leading to well dispersed ferrogels and, at the same time, produce hybrid networks which potentially might show absorption and release capabilities controlled by pH.

As a first and important step in this direction we studied the effects that these PAA-coated NPs have on the structure, thermal properties and swelling capabilities of PVA hydrogels and the effect that the extent of NPs aggregation have on the magnetic properties of the final systems. In all

5

cases we compared the obtained results with equivalent systems obtained using non-coated (only stabilized by charge) magnetic NPs obtained by traditional coprecipitation methods. This allow us to analyze, not only the influence of coating on the dispersion level of obtained nanocomposites, but also the effect of morphology of NPs distribution on the physical (melting temperature, crystallinity degree, crosslinking density) and magnetic properties (magnetization as a function of applied field, coercive field as a function of temperature and Field-Cooling and Zero-Field-Cooling curves) of the obtained ferrogels.

To our knowledge, this is the first time in which this type of poly(electrolyte) coated NPs are used for the synthesis of ferrogels through a non-toxic and environmentally friendly synthesis and processing route.

2. EXPERIMENTAL

Ferrogels were prepared by crosslinking PVA-magnetite aqueous dispersions of different concentrations. Aqueous ferrofluids containing PAA-coated and non-coated NPs with a size of about 10 nm were kindly supplied by NANOGAP Company, Spain. Presence of PAA on the surface of the particles was confirmed by FTIR (see Figure S1 in the supplementary material). Poly (vinyl alcohol) (PVA from Sigma-Aldrich, average molecular weight of 93,500 g/mol and hydrolysis degree of 98-99%) solutions were first prepared by mixing 10 g of polymer and 100 ml of distiller water at 85 °C under continuous stirring for 4 h. After this process, calculated volumes of PAA-coated or non-coated NPs aqueous dispersions (previously sonicated by 30 min, were mixed with 25 ml of the PVA solution to give stable dispersions with approximately 6 wt.% and 9 wt.% of uncoated and coated magnetic NPs, respect to the total content of solids. These dispersions were poured into a mould and frozen for 1h (F,-18 °C). Then, the solution was allowed to thaw at room temperature (T, 25 °C) for the same time. This F-T process was repeated 3 times. Throughout this paper the following nomenclature for samples is used: *6PAA*: ferrogel with 6 wt.% of *PAA*-coated

6

NPs; *9PAA*: ferrogel with 9 wt.% of *PAA*-coated NPs; *6NC*: ferrogel with 6 wt.% of non-coated NPs and *9NC*: ferrogel with 9 wt.% of non-coated NPs.

Field emission scanning electron microscopy (FESEM, Zeiss ULTRA plus instrument) was used to determine the dispersion level of NPs in the matrix. Samples were swollen, frozen, lyophilized and then cryofractured with N_2 liquid before testing. Differential Scanning Calorimetric (DSC) measurements were carried out in a Shimadzu DSC-50 from room temperature to 250 ºC at 10 ºC/min, under N_2 atmosphere. The melting temperature (T_m) and the crystallinity degree were taken from the obtained curve. Before DSC analysis, gels samples were dried for 48 h at 37 ºC. The degree of crystallinity (X_{cr} %) was calculated from the following equation:

$$X_{cr}\% = \frac{\Delta H}{\Delta H^0 \times W_{PVA}} \times 100$$

(1)

where ΔH was determined by integrating the area under the melting peak over the range 190-240 °C and ΔH^0 was the heat (138.6 J/g) required for melting a 100% crystalline PVA sample [45] and W_{PVA} is the mass fraction of the matrix.

To study the possible structures or agglomeration of the NPs within gel, Small-angle X-ray (SAXS) experiments were performed in the SAXS line of the Brazilian Synchrotron Light Laboratory (LNLS).

Thermogravimetric (TGA) studies were performed in a Shimadzu TGA-DTGA 50 from room temperature to 900 ºC at 10 ºC/min under air atmosphere. Degradation temperature (T_p) and iron oxide content, reported as the fully oxidized crystalline phase, Fe_2O_3, (*Fe$_2$O$_3$ wt.%*) were obtained from these measurements.

To perform gel fraction (*GF%*) measurements, a slice of each sample was placed in oven at 37 ºC until no change in its mass was observed. Each sample was immersed into distilled water at room temperature for 4 days to rinse away un-reacted species. Subsequently, the immersed sample was removed from distilled water and dried at 37 ºC until constant weight was reached. Therefore the gel fraction can be calculated as follows:

7

$$GF\% = \frac{W_f - W_F}{W_i - W_F} \times 100 \qquad (2)$$

where W_i and W_f are the weights of the dried hydrogels before and after immersion respectively, and W_F is the weight of the used filler.

Swelling determinations were carried out in saline solution (pH = 7.4) at 25 ºC. All samples were dried before immersion at 37 ºC for 48 h. The equilibrium swelling degree (M_∞ %) was determined by the following equation:

$$M_\infty\% = \frac{M_f - M_i}{M_i} \times 100 \qquad (3)$$

where M_i is the weight of the samples after immersion and M_f is the weight of the sample at equilibrium water content.

Magnetic properties were analyzed using a Superconducting Quantum Interference Device (Quantum Design, MPMS, *XL*). Magnetization curves as a function of applied field were obtained at different temperatures from 5 to 300 K between -20 and 20 kOe. Field-Cooling and Zero-Field-Cooling (*FC/ZFC*) curves were obtained in the temperature range from 5 to 350 K under an external applied field of 50 Oe. Ms values were expressed per gram of uncoated oxide, as emu/g Fe_2O_3.

3. RESULTS AND DISCUSSION

3.1. Morphology of Ferrogels.

Optical images of ferrogels can be observed in **Figure 1** (a, d). A clear difference in homogeneity can be observed between samples prepared with PAA-coated and non-coated NPs pointing to higher extension of aggregation for ferrogels obtained with non-coated fillers (apparent differences in color between coated and non-coated NPs could be associated to a slightly higher level of surface oxidation in the case of PAA-coated NPs that does not seem to have any influence on the magnetic properties of the materials, as will be shown below). This is also observed in FESEM images (Fig. 1) of the fracture surface of ferrogels. Micrographs show the formation of separated micrometric compact

8

aggregates in samples modified with non-coated NPs, whereas samples prepared with PAA-coated NPs present a more homogeneous structure characterized by diffuse NPs clusters arranged on the whole sample. This is probably a consequence of both, improved initial stability of PAA-coated particles in the colloidal dispersion and favorable hydrogen bond interactions between the surface coating (PAA) and PVA chains of the hydrogel [46].

3.2. Thermal Properties and Network Structure.

Several mechanisms have been proposed trying to explain the crosslinking process occurring by F-T. Some authors consider that during freezing stages polymer concentrates in regions between ice crystals, promoting the generation of PVA crystallites. These crystallites would be responsible of gel formation, acting as crosslinking points between PVA chains. Upon thawing stage and melting of ice crystals, a porous matrix would be generated formed by polymer-poor regions embedded in the surrounding polymer-rich gel. During consecutive F-T cycles, ice crystals would tend to preferentially form in the pores, increasing crystallinity degree of the gel, and giving a more resistant material. [1, 9-10] Although this is the general accepted idea, other mechanisms pointing to the possibility of hydrogen bonding as the inducing interaction responsible for the formation of the physical network [35,47] and even the occurrence of chemical crosslinking processes arising from the creation of free radicals formed by shear during ice grow, have been proposed [48].

In any case, presence of NPs could strongly influence both, the formation process of the network and the final properties of the materials. This effect can be even more important for particles stabilized with coatings that can form strong bonds with chemical groups of the host. This is the case of PAA, which presents available carboxylic acid groups in its structure. NPs effect on the network can be revealed by analysis of the thermal and physical properties of the final ferrogels. By analysis of samples with a similar content of Fe_2O_3 $wt.\%$ (11-12 wt%), it is clear that T_p, T_m and X_{cr} increase with the presence of PAA-coated NPs and decrease with the addition of non-coated NPs respect to the neat matrix. (**Table 2**). T_m showed a small increase for PAA-coated based systems

9

respect to the neat PVA hydrogel. On the contrary, addition of non-coated NPs produced a slight decrease on this value. This could be associated with a moderate increase and decrease of the PVA crystal size respect to the hydrogel respectively. Crystallinity also showed a markedly decrease in the case of non-coated systems, whereas the opposite behavior was observed for hydrogels modified with PAA-coated NPs. The effect of the presence of NPs on the degradation temperature of nanocomposites was also important. In the case of ferrogels with a higher level of dispersion (obtained with PAA-coated NPs), T_p increased almost 50ºC respect to the neat hydrogel. This is in agreement with the expected behavior for ferrogels with a good dispersion of NPs in the matrix [49]. As reported by Goiti et al., even small amounts of well dispersed magnetite NPs are effective in shifting T_p to higher values. This effect has been associated to restrictions in polymer chain mobility and reduction of diffusivity of attacking agents within the polymer matrix, both due to the polymer-filler interactions [49].

Results presented above suggest different roles for both kinds of NPs in the matrix. As mentioned, *PAA*-coated NPs can easily form hydrogen bonding through their carboxyl groups with OH groups of PVA [35]. This enables a strong interaction of NPs with the PVA chains even before the crosslinking process starts, i.e. before formation of the gel. It seems possible that the intimate contact between NPs and polymer could facilitate nucleation of big crystals in the PVA matrix, explaining the higher values of X_{cr} and T_m for these nanocomposites respect to unmodified PVA.

The crosslinking density of the gel can be inferred by the *GF%*. As can be seen in table 2, *GF*% did not increase with the presence of *PAA*-coated NPs and shows a marked increase for non-coated NPs. Moreover, swelling increased for the PAA modified samples, and decreased for the non-coated modified systems (with high *GF%*). As described above, models proposed for cryogel formation state that ice crystals formed during the freezing stage promote the generation of PVA crystallites by increasing, locally, the concentration of polymer chains through the formation of "polymer fences" around ice. Then, these crystallites would act as entanglements for pendant chains bridging the neighbouring crystallites [9]. Within this framework, results obtained for systems

10

modified with PAA-coated NPs are unexpected. The increase in X_{cr} observed for *PAA*-coated NPs gels did not seem to affect the crosslinking density of the system. This would indicate that crystalline regions in the PVA could be acting as physical crosslinks but only to a small degree. Formation of a heterogeneous dispersion of big crystals in the network would produce an increase in the crystallinity degree and melting temperature of the system, with a poor contribution to the physical gelation of PVA, explaining the observed results. On the other hand, some authors [35,47] have claimed that the predominant factor in the gelation of PVA hydrogels is the formation of physical crosslinks by hydrogen bonding between hydroxyl groups of PVA and not the formation of crystallites. In presence of PAA, an increase in hydrogen bonding between PAA-coated NPs (plenty of carboxylic groups) and PVA chains could be expected to occur, at expenses of a decrease in hydrogen bond self-association between PVA chains. However, the extent in which the interaction between *PAA*-coated NPs and PVA can contribute to the formation of crosslinked regions is, at this point, not completely understood.

In the case of non-coated NPs, the high increase in the *GF*% and the decrease in the $M_{\infty}\%$ indicate that these gels are more crosslinked than the matrix. However, X_{cr} decreased. We propose that NPs aggregates formed in this system from the very beginning of processing could be acting as additional physical crosslinking points conducting to a less crystalline matrix but to a more crosslinked ferrogel.

It is important to note that ferrogels obtained using PAA-coated NPs showed an important increase in swelling respect to the neat matrix (almost 50%). This effect is probably a consequence of the presence of carboxylate groups on the surface of magnetic NPs. At physiological pH (7.4), most of carboxylic groups are present as carboxylate anions. Under these conditions, electrostatic repulsion between ions of the same charge and the osmotic imbalance between the interior and exterior of the gels cause further expansion of the 3D polymer network [50] similar extra expansions have been observed for cationic polymer gels when environmental pH decreases below a critic value [39]. Hence, by the only addition of PAA-coated NPs and without the use of any other

11

comonomer, PVA hydrogel was transformed in a ferrogel with improved swelling ability, crystallinity and degradation temperature and potential pH-responsive characteristics. All these results would indicate that PVA/PAA-coated NPs based ferrogels could be very interesting candidates for drug delivery and other biomedical applications.

3.3. SAXS experiments.

Small-angle X-ray scattering (SAXS) is a powerful technique to determine structural organization of NPs in a polymer matrix and has been already successfully used in the analysis of ferrogels [51-53].

In this work, SAXS was used as a semi-quantitative tool for the structural and comparative analysis of coated and non-coated NPs dispersions in PVA hydrogels. Although the restricted range of the obtained SAXS spectra does not allow performing a comprehensive study of the real ferrogels structure, some general trends can be obtained, useful for a comparative and semi-quantitative analysis. Figure 2 shows the Log-Log plot of I(q) vs q for ferrogels obtained with PAA and non-coated NPs. SAXS experimental curves display three and two different scattering regions, respectively. The existence of a third power-law regime describing agglomerates has already been observed by Hernandez et al. [53].At low q values, both samples showed a power-law dependency of the SAXS intensity of the form $I(q) = I_0 q^{-\alpha}$, where I_0 is a constant and α is related to the correlation length on the material (which can be determined from the slope of the linear part of the Log-Log plots) [54]. For samples obtained with non-coated NPs, the low q region has a slope of -1.3 and -1.5, for 6 wt.% and 9 wt.% respectively, values that are close to those reported for dilute ferrofluids suspended in polymer gels [55].

Using Guinier formula $I(q)=Gexp(-q^2 R_g^2/3)$ where G is the Guinier prefactor, we calculated the radius of gyration, R_g, of the scattering objects [56]. The obtained values were approximately 19 and 11 nm for systems modified with coated and non-coated NPs respectively. Assuming that shape of the largest dispersed structure is a sphere, and using $D = 2(5/3)^{1/2}R_g$ (where D is the diameter of

12

the object), we obtained sizes of approximately 49 nm for samples modified with PAA-coated NPs and 28 nm for gels with non-coated NPs. Both values are greater than the size of the individual NPs. These values are presented in **Table 1.** Based on these preliminary results, and considering FESEM images, samples could be represented as formed by a distribution of micrometric NPs aggregates constituted by smaller NPs clusters. The nature of these aggregates (distance between particles, shape, etc.) seems to depend on the nature of NPs coating. In the case of non-coated samples, big aggregates are compact and form well defined NPs rich zones in the matrix. This is probably a consequence of the absence of coating that induces aggregation and close contact between NPs. On the other hand, PAA-coated NPs, with a stronger affinity by PVA, form smaller, more diffuse aggregates (larger separation between NPs) distributed in the whole sample (see Figs. 1 e-f). This behaviour points to a lower tendency to aggregation for PAA-coated NPs in the PVA gel which is attributed to the stabilizing effect of PAA and its strong interactions with the PVA matrix.

In the high q-regime (Porod regime) all samples show a decay of the scatter intensity with q^{-4} characteristic of Porod scattering from sharp interfaces and related to the individual particles [57]. As we mentioned previously, in the case of samples with PAA-coated NPs, three linear regions are identified while for ferrogels with non-coated NPs only two regions are observed. We associated these difference on the α value to different correlation scales on the characteristic length in the material. Hence, it would indicate that in samples with PAA-coated NPs different structures, related with different length scales, coexist.

To facilitate the analysis we replot the data of figure 2 as $q^4 I(q)$ *vs.* q (see inset). In the scattering profile of samples modified with PAA-coated NPs, a well defined peak can be distinguished, whereas in samples modified with non-coated NPs two peaks are observed. The first peak gives a value of about 7.2 and 7.7 nm for samples prepared with coated and non-coated NPs respectively (for q range values where $\alpha = 4$), and is mainly associated with the size of NPs in the clusters. The second peak observed for samples prepared with non-coated NPs (at lower value of q and below the characteristic q values of particles sizes) is associated to the cluster size. From this

13

peak, a value of approximately 40 nm was obtained, consistent with the Guinier approximation and, as we will see later, in complete correspondence with the magnetic properties.

For samples modified with PAA-coated NPs a peak for low values of q was not observed. This could be because of the low compactness of the sample which is associated with a low intensity of the scattered wave (not observed) or because the value of q is below the lowest measured (see [53]). In summary, both FESEM and SAXS experiments show that samples were formed by micrometric aggregates dispersed in the matrix, and that these aggregates are constituted by smaller NPs clusters. Samples prepared with non-coated NPs seem to present a more compact and less branched internal structure than aggregates formed by PAA-coated NPs, i.e. the distance between NPs in samples prepared with PAA-coated NPs would be greater than in the case of aggregates formed by non-coated NPs. This is clearly a consequence of the presence of the PAA coating on the surface of NPs.

3.4. Magnetic Properties.

As described above, PAA-coated ferrogels showed a higher level of dispersion when compared with systems obtained with non-coated NPs. However, as extent of aggregation, formation of aggregates and distance between NPs in the clusters can strongly influence the magnetic properties of ferrogels, the study of the real magnetic response of final materials is of paramount importance.

Magnetization hysteresis loops of the samples were obtained at two different temperatures (5 and 300 K) at a maximum applied field of 20 kOe (**Figure 3**). All samples measured at room temperature showed a relatively high saturation magnetization (M_S). These asymptotic values are 50.1, 50.0, 50.1 and 50.0 emu/g Fe_2O_3 for samples 6*PAA*, 9*PAA*, 6*NC* and 9*NC*, respectively. These values are smaller than expected for well–crystallized bulk Fe_3O_4 with a *Ms* of 90 emu/g [58]. Decrease in *Ms* respect to the bulk value could be a consequence of different contributions like surface disorder and low crystallinity that explain the large variability of Ms values found in the

14

literature between samples obtained by different procedures and under different conditions. For example, Xu et al. [40] have published M_s values of approximately 82 emu/g for PAA-coated magnetite nanoparticles (50 nm). Lima et al. have reported *Ms* values of 80 emu/g for NPs with a size of 7 nm [59] whereas Ms values near to 20 emu/g were also found for 5 nm magnetite NPs [60]. Iron oxide magnetite NPs with average sizes of 4.5 nm and 6 nm Ms show *Ms* values of 20 emu/g and 58 emu/g respectively [61]. *Ms* between 55 and 65 emu/g for 20 nm magnetite NPs have also been found [62]. Hence, considering that in our case nanoparticle nominal size is about 10 nm in diameter, the obtained M_S value would indicate that surface effects and/or low crystallinity are playing an important role on magnetization.

A zoom of the magnetization loops at 5 and 300 *K* are shown in the inset of figure 3 in order to display coercive field values. As expected, a marked increase in the coercive field (H_C) as the temperature decreases can be observed. This is the typical behavior expected for superparamagnetic systems in which, at low temperatures (below the blocking temperature), magnetic relaxation time is longer than measurement time, the system is thermally blocked and the coercive field has a value different from zero. For higher temperatures, the magnetic relaxation time is shorter than the measurement time and the particles ensembles are considered as a "paramagnetic" system (see Hc values in table 3). At T = 300 *K* all samples exhibit low coercive fields, typical of superparamagnetic systems with weak interactions between NPs [21]. However, a slight difference between samples prepared with PAA-coated NPs and non-coated NPs can be noticed. Ferrogels obtained with PAA-coated NPs show H_C values around 10 Oe, while samples with non-coated NPs show values around 20 Oe. In the case of PAA samples, smaller H_C values obtained at room temperature can be explained by a better dispersion, less interaction between NPs and a superparamagnetic behavior. This difference was more pronounced at low temperatures, with NPs in the blocked state. At T=5K, coercive field values associated to 6PAA and 9PAA samples were about 140 Oe, whereas values of 298 and 282 Oe were obtained for 9NC and 6NC samples, respectively (see table 3). These differences are a consequence of the higher magnetic interactions

15

present in NC samples due to the formation of micrometric aggregates and is in agreement with ZFC/FC results discussed later. Thus, PAA coating reduces the interaction between NPs and promotes a more homogeneous distribution of NPs in PVA.

As can be seen in fig. 3 a concentration increase does not seem to affect magnetostatic properties, such as saturation magnetization or coercive field. This is observed in **Table 3** for both kinds of ferrogels (PAA and NC gels).

Figure 4 shows the coercive field as a function of temperature for two of the samples. For samples prepared with PAA-coated NPs, Hc decreases from about 140 Oe at 5 K to nearly 10 Oe at room temperature. At temperatures below 50 K the coercive field depends on $T^{0.5}$ which is typical for a random distribution of anisotropies. Above 50 K the H_C separates from the expected dependency with $T^{0.5}$.

ZFC/FC measurements, displayed in **Figure 5** and **6**, were carried out in the following way: the sample was first cooled down from 300 to 5 K without magnetic field, then a static magnetic field of 50 Oe was applied and the magnetization values were measured increasing the temperature up to 350 K (ZFC measurement). Then, the sample was cooled down to 5 K under applied magnetic field (50 Oe) and, again, magnetization values taken in a heating scan from 5 to 350 K (FC curve).

From the *ZFC* curve blocking temperature (T_B) can be determined, defined as the maximum of the *ZFC* curve, being 128 K for samples 6PAA and 9PAA, which proves the superparamagnetic behavior of these ferrogels. In samples prepared with non-coated NPs the blocking temperature seems to be above room temperature.

The irreversibility temperature, T_i (defined as the threshold temperature above which *FC* and *ZFC* curves coincide) was about 152 K for both samples. The small difference between the maximum of the *ZFC* curve (T_B) and T_i (around 34 K) is related to the low polydispersity of these NPs (a narrow distribution of blocking temperatures is related with a narrow energy barrier distribution) [21,63].

16

Under the assumption that coated-magnetic NPs inside the PVA gel are only weakly interacting, the estimation of T_B allows the assessment of the mean energy barrier (E_B). This can be done using the usual equations $T_B = K_{eff} V/25k_B$ and $E_B = K_{eff}V$ [21] and the particle nominal diameter of 10 nm, from which we obtained $E_B = 4.5\text{x}10^{-20}$ J ($4.5\text{x}10^{-13}$ erg) and an effective anisotropy constant $K_{eff} = 8.5\text{x}10^5$ erg/cm^3 or *PAA* samples. These values are in good agreement with values reported in the literature for similar systems [64-67].

In the NC samples the ZFC/FC curves have similar characteristics to that observed in percolated clusters glasses, in which a "shoulder" is seen at low temperatures, instead of a peak [21, 68-69]. This can be associated with the formation of compact clusters and an increase of interactions between NPs. The magnetization intensity of the *9NC* samples is greater than the *6NC* samples due to the difference in concentration of magnetite NPs used in the synthesis.

4. CONCLUSIONS

Superparamagnetic ferrogels with high X_{cr}, T_m, T_p and high swelling ability could be obtained using a non-toxic and environmentally friendly procedure based on physical crosslinking of aqueous dispersions of PVA/PAA-coated magnetite NPs by freezing-thawing.

Ferrogels prepared with PAA-coated NPs show a much more homogeneous distribution of the filler (organized in diffuse NPs clusters) than samples prepared with non-coated NPs, as demonstrated by FESEM and SAXS experiments. Both magnetic and structural characterization evidenced that PAA coating promotes interaction between NPs and the matrix (probably by hydrogen bonding) improving homogeneity of the ferrogels. More important, the presence of PAA-coated NPs induced an increase in the swelling capacity of the ferrogel at physiological pH, respect to the neat hydrogel, without precluding their thermal properties. This effect could be of importance in the design of new solvent absorbers and stimuli-responsive drug delivery devices formed through a non-toxic and environmentally friendly procedure. This approach could be extended to other NPs and polyelectrolytes systems, enhancing the range of applications of functional nanocomposites.

17

5. ACKNOWLEDGEMENTS

6. REFERENCES

[1] Hassan CM, Peppas NA. Structure and applications of poly(vinyl alcohol) hydrogels produced by conventional cross-linking or by freezing/thawing methods. Adv Polym Sci. 2000;153:37–65.

[2] Osada Y, Gong JP, and Tanaka YJ. Polymer gels. J Macromol Sci Polymer Rev. 2004;44(1):87–112.

[3] Sonmez HB and Wudl F. Cross-linked poly(orthocarbonate)s as organic solvent sorbents. Macromolecules 2005;38(5):1623-1626.

[4] Guvendiren M, Lu HD and Burdick JA. Shear-thinning hydrogels for biomedical applications. Soft Matter 2012;8(2):260-272.

[5] Lee KY and Mooney DJ. Alginate: Properties and biomedical applications. Prog. Polym Sci. 2011; 37(1):106-126.

[6] Seliktar D. Designing Cell-Compatible Hydrogels for Biomedical Applications. Science 2012; 336:1124-1128.

[7] Fernández-Barbero A, Suárez IJ, Sierra-Martín B, Fernández-Nieves A, Javier de las Nieves F, Marquez M, Rubio-Retama J and López-Cabarcos E. Gels and microgels for nanotechnological applications. Adv. Colloid Interfac. 2009;147–148:88–108.

[8] Park MH, Joo MK, Choi BG and Jeong B. Biodegradable Thermogels. Accounts Chem. Res. 2012; 45(3):424–433.

[9] Willcox PJ, Howie JrDW, Schmidt-Rohr K, Hoagland DA, Gido SP, Pudjianto S, Kleiner LW and Vancatraman S. Microstructure of poly(vinyl alcohol) hydrogels produced by freeze/thaw cycling. J. Polym Sci Pol Phy. 1999;37(24):3438-3454.

[10] Ricciardi R, Auriemma F, Gaillet C, De Rosa C and Laupretre F. Investigation of the Crystallinity of Freeze/Thaw. Poly(vinyl alcohol) Hydrogels by Different Techniques. Macromolecules 2004;37(25):9510-9516.

[11] Gonzalez JS, Hoppe CE and Alvarez VA. Poly (vinyl alcohol) ferrogels: synthesis and applications. In: Wythers MC, editor. Advances in Materials Science Research. Vol.13. chapter 8, Nova Science Publishers, Inc. New York, 2011.

[12] Zrínyi M. Colloidal particles that make smart polymer composites deform and rotate. Colloids Surfaces A 2011;382(1-3):192–197.

[13] Filipcsei G, Csetneki I, Szilágyi A and Zrínyi M. Magnetic Field-Responsive Smart Polymer Composites. Adv Polym Sci 2007;206:137–189.

[14] Galicia JA, Cousin F, Dubois E, Sandre O, Cabuil V and Perzynski R. Static and dynamic structural probing of swollen polyacrylamide ferrogels. Soft Matter 2009;5:2614-2624.

[15] Galicia JA, Cousin F, Dubois E, Sandre O, Cabuil V, Perzynski R. Local structure of polymeric ferrogels. J. Magn Magn Mater. 2011;323(10):1211–1215.

[16] Chen MC, Liang HF, Chiu YL, Chang Y, Wei HJ and Sung AW. A novel drug-eluting stent spray-coated with multi-layers of collagen and sirolimus. J. Control Release 2005;108(1):178-189.

[17] Berry CC. Possible exploitation of magnetic nanoparticle–cell interaction for biomedical applications. J Mater Chem, 2005;15:543-547.

[18] Hernández R, Sacristán J, Mijangos C, Asín L, Torres TE, Ibarra MR and Goya GF. Magnetic Hydrogels Derived from Polysaccharides with Improved Specific Power Absorption: Potential Devices for Remotely Triggered Drug Delivery. J Phys Chem B 2010;114:12002-12007.

[19] Lim S, Lee S-W. Fabrication of Triple-Layered Magnetite-Hydrogel-Gold Nanocomposites for Biomedical Applications. J Nanosci Nanotech. 2012;12(2):1242-1245.

[20] Daniel-da-Silva AL, Trindade T, Goodfellow BJ, Costa BFO, Correia RN and Gil AM. In Situ Synthesis of Magnetite Nanoparticles in Carrageenan Gels. Biomacromolecules 2007;8:2350-2357.

[21] M. Knobel, W. C. Nunes, L. M. Socolovsky, E. De Biasi, J. M. Vargas and J. C. Denardin. Superparamagnetism and Other Magnetic Features in Granular Materials: A Review on Ideal and Real Systems. J Nanosci Nanotech, 2008;8:2836 – 2857.

[22] De Biasi E, Ramos CA, Zysler RD and Romero H. Large surface magnetic contribution in amorphous ferromagnetic nanoparticles. Phys Rev B 2002;65:144416- 144424.

[23] Wilcoxon JP, Venturini EL and Provencio P. Magnetic response of dilute cobalt nanoparticles in an organic matrix: The effects of aging and interface chemistry. Phys Rev B 2004;69:172402-172406.

[24] Pankhurst QA, Yedra Martinez A and Fernandez Barquin L. Interfacial exchange pinning in amorphous iron-boron nanoparticles. Phys. Rev. B 2004;69:212401-212405.

[25] Ledo Suarez A, Puig J, Zucchi IA, Hoppe CE, Gomez ML, Zysler R, Ramos C, Marchi MC, Bilmes SA, Lazzari M, Lopez Quintela MA and Williams RJJ. Functional nanocomposites based on the infusion or in situ generation of nanoparticles into amphiphilic epoxy gels. J. Mater. Chem 2010;20:10135–10145.

[26] Bajpai AK, Gupta R. Synthesis and characterization of magnetite (Fe3O4)—Polyvinyl alcohol-based nanocomposites and study of superparamagnetism. Polym Composites 2010; 31:245–255.

[27] Scotchford CA, Cascone MG, Downes S, Giusti P. Osteoblast responses to collagen-PVA bioartificial polymers in vitro: the effects of cross-linking method and collagen content. Biomaterials 1998;19(1-3):1-11.

[28] Guo Z, Zhang D, Wei S, Wang Z, Karki AB, Li Y, Bernazzani P, Young DP, Gomes JA, Cocke DL and Ho TC. Effects of iron oxide nanoparticles on polyvinyl alcohol: interfacial layer and bulk nanocomposites thin film. J Nanopart Res 2010;12:2415–2426.

[29] Gries K, Vieker H, Gölzhäuser A, Agarwal S and Greiner A. Preparation of Continuous Gold Nanowires by Electrospinning of High-Concentration Aqueous Dispersions of Gold Nanoparticles. Small 2012; 8(9):1436-1441.

[30] Lee J, Isobe T and Senna M. Magnetic properties of ultrafine magnetite particles and their slurries prepared via in-situ precipitation. Colloids Surface A. 1996;109:121–127.

[31] van der Zande BMI, Pages L, Hikmet RAM and van Blaaderen A. Optical Properties of Aligned Rod-Shaped Gold Particles Dispersed in Poly(vinyl alcohol) Films. J. Phys. Chem. B 1999;103 (28):5761-5767.

[32] Hernández, D López, M Vázquez, C Mijangos. Magnetic characterization of polyvinyl alcohol ferrogels and films. J Mater Res 2007;22:2211-2216.

[33] Pana O, Craciunescu I, Mijangos C, Goiti E, Soran ML, Turcu R, Chauvet O. Magnetic Composites between core- shell Fe@Au nanoparticles and polymers. J. Nanostructured Polym. Nanocomposites 2007;3(3):96-102.

[34] Lin H, Watanabe Y, Kimura M, Hanabusa K and Shirai H. Preparation of magnetic poly(vinyl alcohol) (PVA) materials by in situ synthesis of magnetite in a PVA matrix. J Appl Polym Sci. 2003;87(8):1239–1247.

[35] Gann McMJ, Higginbotham CL, Geever LM, Nuget MJD. The Synthesis of Novel pH-sensitive Poly(Vinyl Alcohol) Composite Hydrogels Using a Freeze/thaw Process for Biomedical Applications. Int J Pharm, 2009;372:154-161.

[36] Kim B and Peppas NA. In vitro release behavior and stability of insulin in complexation hydrogels as oral drug delivery carriers. Int J Pharm 2003;266:29–37.

[37] Jin X and Hsieh YL. pH-responsive swelling behavior of poly(vinyl alcohol)/poly(acrylic acid) bi-component fibrous hydrogel membranes. Polymer 2005;46(14):5149–5160.

[38] Smith TJ, Kennedy JE and Higginbotham CL. Rheological and thermal characteristics of a two phase hydrogel system for potential wound healing applications. J Mater Sci 2010;45(11):2884– 2891.

[39] Lu Y, Wang D, Li T, Zhao X, Cao Y, Yang H and Duan YY. Poly(vinyl alcohol)/poly(acrylic acid) hydrogel coatings for improving electrode-neural tissue interface. Biomaterials 2009;30(25):4143–4151.

[40] Xu YY, Zhou M, Geng HJ, Hao JJ, Oua QQ, Qi S-D, Chen H-L and Chen X-G. A simplified method for synthesis of Fe3O4@PAA nanoparticles and its application for the removal of basic dyes. Appl Surf Sci. 2012;258(8):3897– 3902.

21

[41] Ersenkal DA, Ziylan A, Ince NH, Acar HY, Demirer M and Copty NK. Impact of dilution on the transport of poly(acrylic acid) supported magnetite nanoparticles in porous media. J. Contaminant Hydrology 2011;126(3-4):248-257.

[42] Yang X, Jiang W, Liu L, Chen B, Wu S, Sun D and Li F. One-step hydrothermal synthesis of highly water-soluble secondary structural Fe3O4 nanoparticles. J. Magn Magn Mater. 2012:324(14):2249-2257.

[43] Isojima T, Lattuada M, Vander Sande JB, Hatton TA. Reversible Clustering of pH- and Temperature-Responsive Janus Magnetic Nanoparticles. ACS Nano 2008;2(9):1799-1806.

[44] M. Lattuada, T.A. Hatton. Preparation and Controlled Self-Assembly of Janus Magnetic Nanoparticles. J. Am. Chem. Soc. 2007;129(42):2878-89.

[45] Peppas NA and Merrill EW. Differential scanning calorimetry of crystallized PVA hydrogels. J Appl Polym Sci 1976;20(6):1457-1465.

[46] Yap HP, Quinn JF, Cho SMNgJ and Caruso F. Colloid surface engineering via deposition of multilayered thin films from polyelectrolyte blend solutions. Langmuir 2005;21(10):4328-4333.

[47] Sinclair GW and Peppas NA. Analysis of non-Fickian Transport in Polymers Using Simplified Exponential Expression. J Membrane Sci 1984;17:329- 331.

[48] Hernandez R, Lopez D, Mijangos C, Guenet JM. A reappraisal of the 'thermoreversible' gelation of aqueous poly(vinyl alcohol) solutions through freezing–thawing cycles. Polymer 2002;43(21):56-61

[49] Goiti E, Salinas M, Arias G, Puglia D, Kenny J and Mijangos C. Effect of magnetic nanoparticles on the thermal properties of some hydrogels "Kinetic study of the termal degradation process of polyvinyl alcohol ferrogels. Polym Degrad Stabil 2007;92(12):2198-2205.

[50] Ohmine I and Tanaka T. Salt effects on the phase transition of ionic gels. J. Chem. Phys. 1982;77 (11):5725–5729.

[51] Hernández R, Nogales A, Ezquerra T and Mijangos C. Structural Organization of Iron Oxide Nanoparticles Synthesized Inside Hybrid Polymer Gels Derived from Alginate Studied with Small-Angle X-ray Scattering Langmuir, 2009; 25 (22):13212-13218.

[52] Hernández R, Nogales A, Ezquerra T and Mijangos C. In situ synthesis of magnetic iron oxide nanoparticles in semi-interpenetrating polymer networks derived from alginate. Influence of the network morphology. Polymer Preprints 2009;50(2):283.

[53] Hernández R, Sacristán J and Mijangos C. Effect of polymer nanoparticle interaction of the structure and reinforcement of hybrids ferrogels derived from alginate. Soft Matter 2010;6(16) 3910-3917.

[54] Beaucage G, Kammler HK and Pratsinis SE. Particle size distributions from small-angle scattering using global scattering functions. J Appl Crystallogr 2004;37:523-535.

[55] Teixeira AV, Morfin I, Ehrburger-Dolle F, Rochas C, Geissler E, Licinio P, Panine P. Scattering from dilute ferrofluid suspensions in soft polymer gels. Phys. Rev. E 2003;67(2):021504.

[56] Guinier A and Fournet G, Small-Angle Sacattering of X-Rays, John Wiley & Sons Inc, New York, 1955.

[57] Glatter O, Kratky O. Small angle X ray scattering; Academic Press: London, 1982.

[58] O'Handley RC, Modern Magnetic Material: Principles and Applications, Wiley Interscience, New York, 2000.

[59] Lima E Jr., De Biasi E, Mansilla M, Vasquez Saleta ME, Effenberg F, Rossi LM, Cohen R, Rechenberg HR and Zysler RD. Surface effects in the magnetic properties of crystalline 3 nm ferrite nanoparticles chemically synthesized. J Appl Phys 2010;108(10):103919-103929.

[60] Vargas JM, Lima JrE, Zysler RD, Duque JGS, De Biasi E and Knobel M. Effective anisotropy field variation of magnetite nanoparticles with size reduction. Eur Phys J B 2008;64(2):211– 218.

[61] Laurent S, Forge D, Port M, Roch A, Robic C, Vander Elst L and Muller RN. Magnetic iron oxide nanoparticles:Synthesis, stabilization, vectorization, physicochemical characterizations and biological applications. Chem Rev 2008;108(6):2064–2110.

[62] Majewski P and Thierry B. Functionalized Magnetite Nanoparticles—Synthesis, Properties, and Bio-Applications Functionalized Magnetite Nanoparticles—Synthesis, Properties, and Bio-Applications. Crit Rev Solid State 2007;32(3-4):203-215.

23

[63] Bonacchi D, Caneschi A, Dorignac D, Falqui A,Gatteschi D, Rovai D, Sangregorio C and Sessoli R. Nanosized Iron Oxide Particles Entrapped in Pseudo-Single Crystals of γ-Cyclodextrin Chem Mater 2004;16(10):2016-2020.

[64] Goya GF, Berquó TS, and Fonseca FC, Morales MP. Static and dynamic magnetic properties of spherical magnetite nanoparticles. J Appl Phy 2003;94(5):3520-3528.

[65] Hoppe CE, Rivadulla F, Vidal Vidal J, López Quintela MA and Rivas J. Magnetic Relaxation of Fe2O3 Nanoparticles Arrangements and Electronic Phase-Segregated Systems. J. Nanosci. Nanotechnol. 2008;8(6): 2883-2890.

[66] Nunes WC, Folly WSD, Sinnecker JP and Novak MA. Temperature dependence of the coercive field in single-domain particle systems. Phys Rev B 2004;70(1):014419.

[67] Hoppe CE, Rivadulla F, López-Quintela MA, Buján MC, Rivas J, Serantes D and Baldomir D. Effect of Submicrometer Clustering on the Magnetic Properties of Free-Standing Superparamagnetic Nanocomposites. J Phys Chem C 2008;112(34):13099–13104.

[68] Sarkissian BVB. The appearance of critical behaviour at the onset of ferromagnetism in AuFe alloys. J Phys F Met Phys 1981;11(10):2191-2208.

[69] Socolovsky LM, Sánchez FH and Shingu PH. Magnetic structure of FexCu100-x magnetoresistive alloys produced by mechanical alloying, Hyperfine Interact 2001;133(1-4):47-52.

FIGURE CAPTIONS

Figure 1: Photograph of a) NC-ferrogels (left *6NC*, right *9NC*) d) PAA-ferrogels (left *6PAA*, right *9PAA*) and FESEM images of b) *6NC* c) *9NC* e) *6PAA* and f) *9PAA*.

Figure 2: *Log-Log* plot of small angle X-ray scattering curves of the four samples (a) 6*PAA* and 9*PAA* (b) 6*NC* and *9NC*. Inset $I(q)$ q^4 *vs. q* for the four samples is shown in the inset.

Figure 3: (a) - (d) show the magnetization vs. field (*M* vs. *H*) hysteresis loop at 5, 200 and 300 *K* for (a) *6PAA*, (b) *9PAA*, (c) *9NC* and (d) *6NC* samples. The insets of the all figures show a zoom in the region -400 Oe ≤ *H* ≤ 400 Oe to observe the difference in the coercive field at *T* = 5 K and *T* = 300 K.

Figure 4: Experimental coercive field versus temperature for a *6NC* and *6PAA* samples.

Figure 5: Zero field cooled and field cooled measured for *6PAA* and *9PAA* samples.

Figure 6: Zero field cooled and field cooled measured for *6NC* and *9NC* samples.

**Table 1**. Values of radius of gyration R_g and size D of the structures inside the PVA matrix

	6PAA	9PAA	6NC	9NC
R_g (*nm*)	19.0 ± 0.5	19.0 ± 0.5	11.0 ± 0.6	11.0 ± 0.6
D (*nm*)	49.0 ± 0.5	49.0 ± 0.5	28.0 ± 0.6	28.0 ± 0.6

Table 2. Thermal and swelling properties of ferrogels.

Gel	Fe_2O_3 % TGA	T_p °C TGA	T_m °C DSC	X_{cr} % DSC	M_∞ %	GF %
matrix	0	284.3±5.3	220.5±0.3	31.80±3.22	221.50±5.36	67.30±3.55
9PAA	15.95±0.04	331.5±5.1	227.3±0.7	45.90±5.0	332.21±32.5	67.32±2.00
6PAA	11.05±0.10	323.5±4.6	226.6±0.2	55.04±4.23	323.02±11.5	68.30±1.15
6NC	11.84±1.05	262.0±6.1	217.8±0.9	25.24±1.60	158.7±3.18	88.37±1.05
9NC	24.9±2.20	255.4±8.8	218.3±0.2	19.07±0.20	204.3±11.3	82.32±2.10

Table 3. Hc and Ms values in samples 6PAA, 9PAA, 9NC and 6NC for 5 and 300 K

Sample	6PAA		9PAA		9NC		6NC	
T (K)	5	300	5	300	5	300	5	300
Hc (Oe)	140.2	11.6	139.5	12.2	298.9	21.0	282.9	19.3
Ms (emu/g)	57.2	50.1	58.1	50.0	57.2	50.0	56.5	50.1

Figure 1

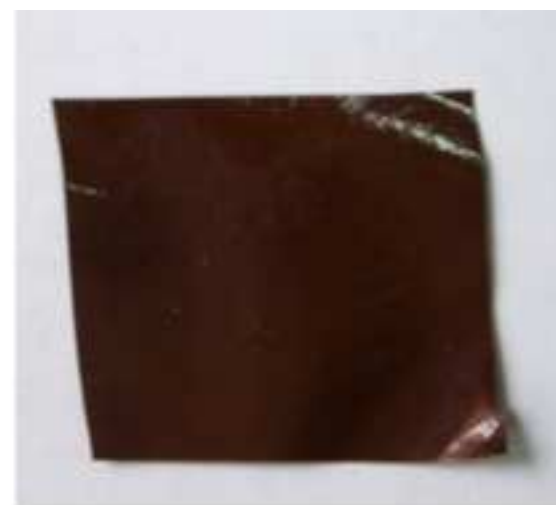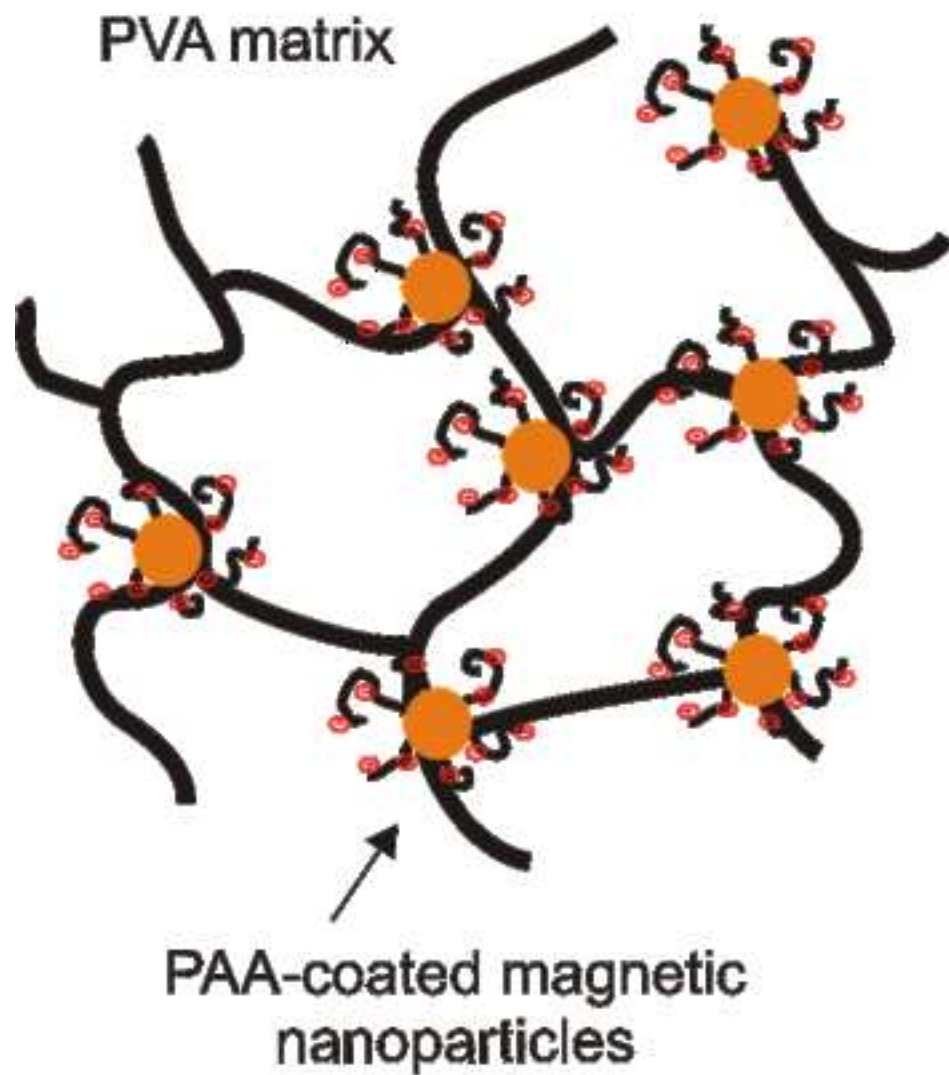**Figure 2**

Figure 3
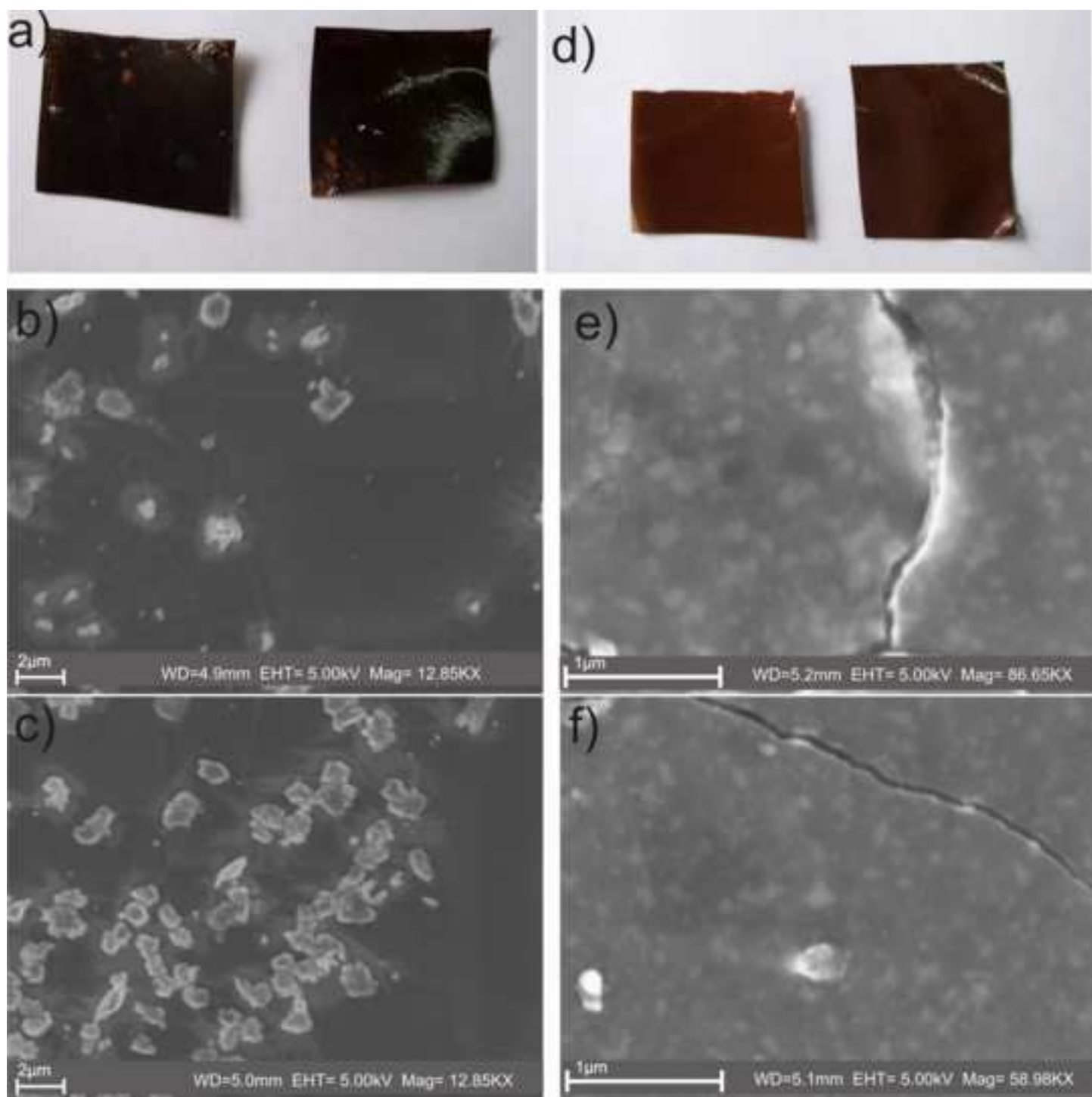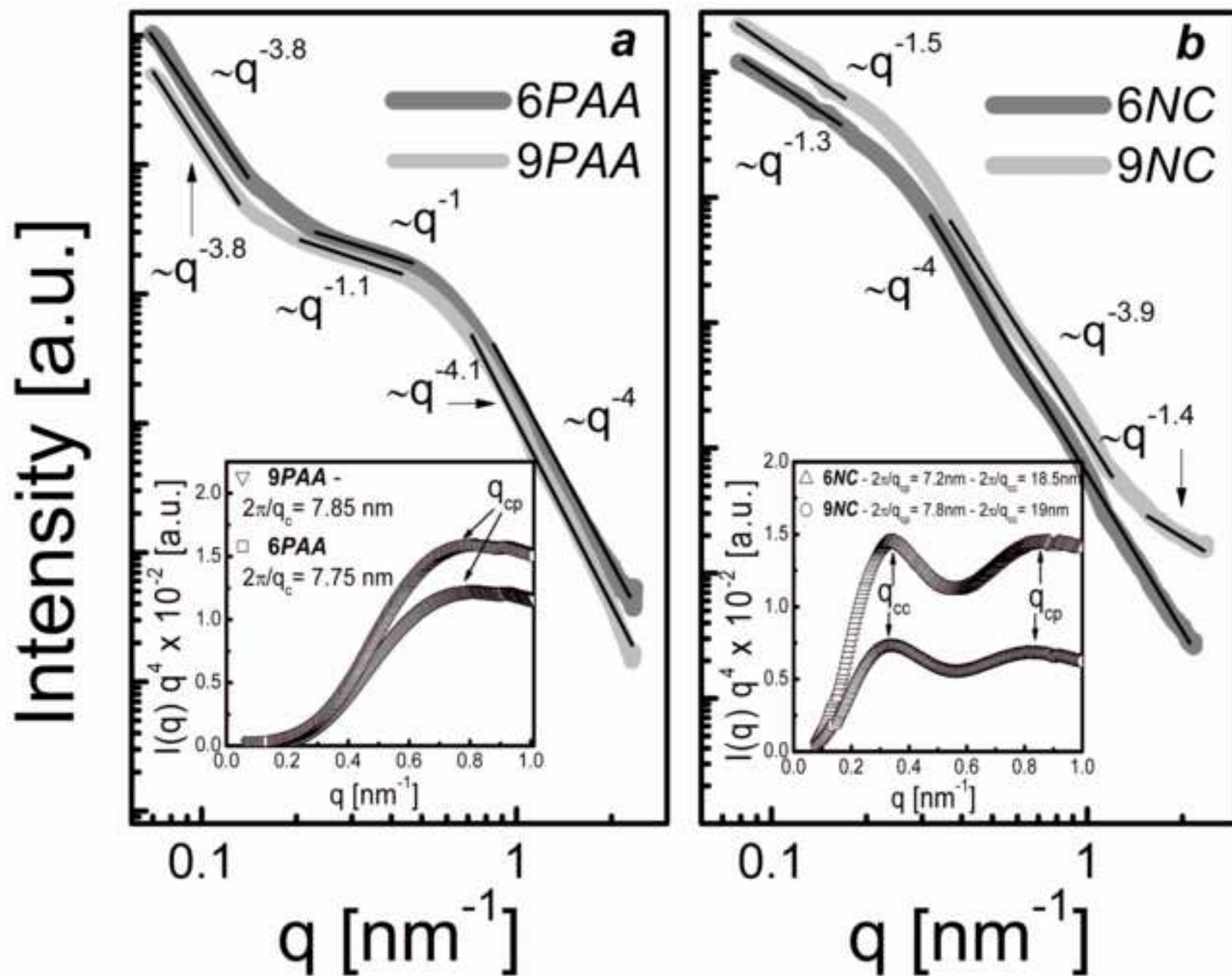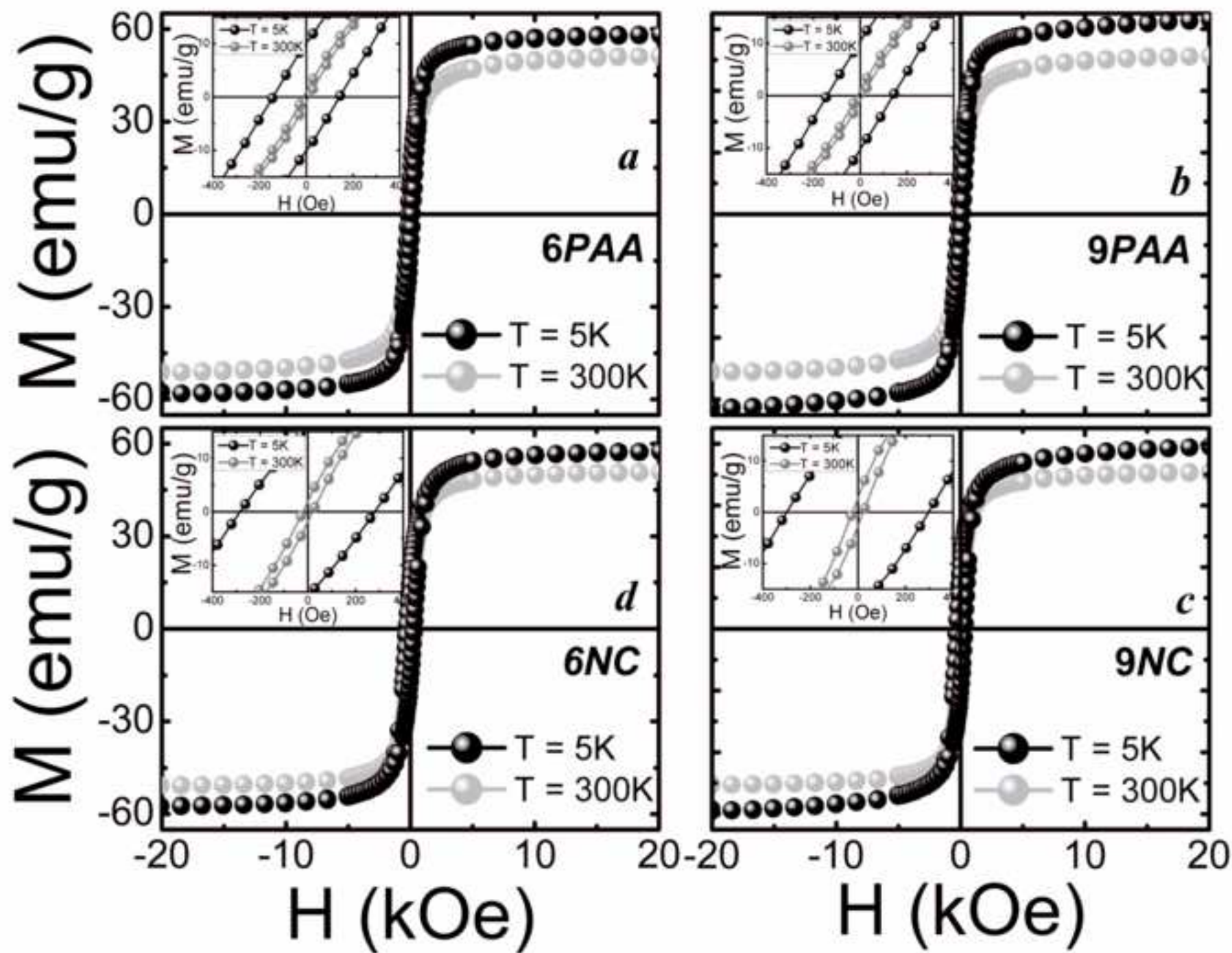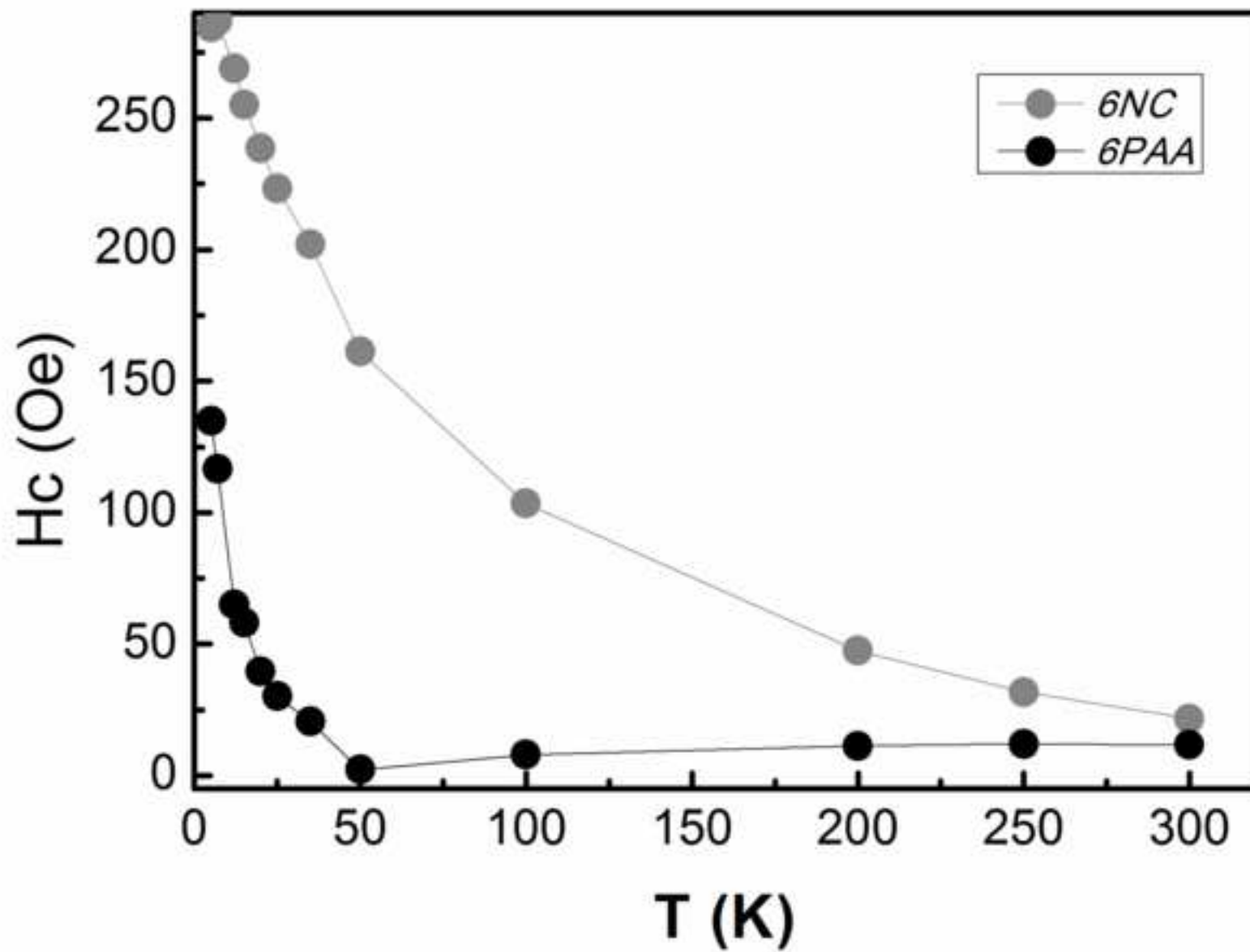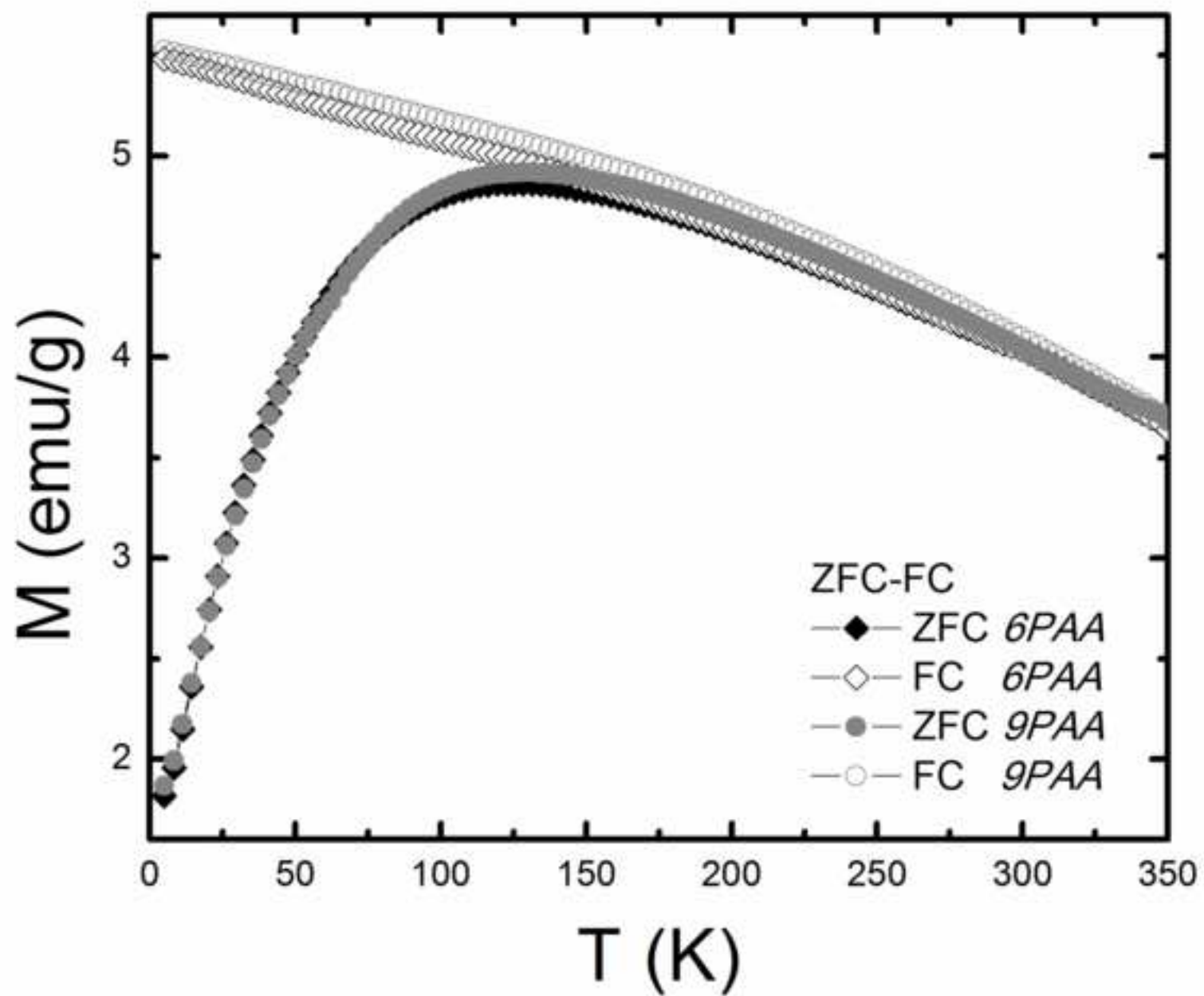
Figure 4

Figure 5

Figure 6
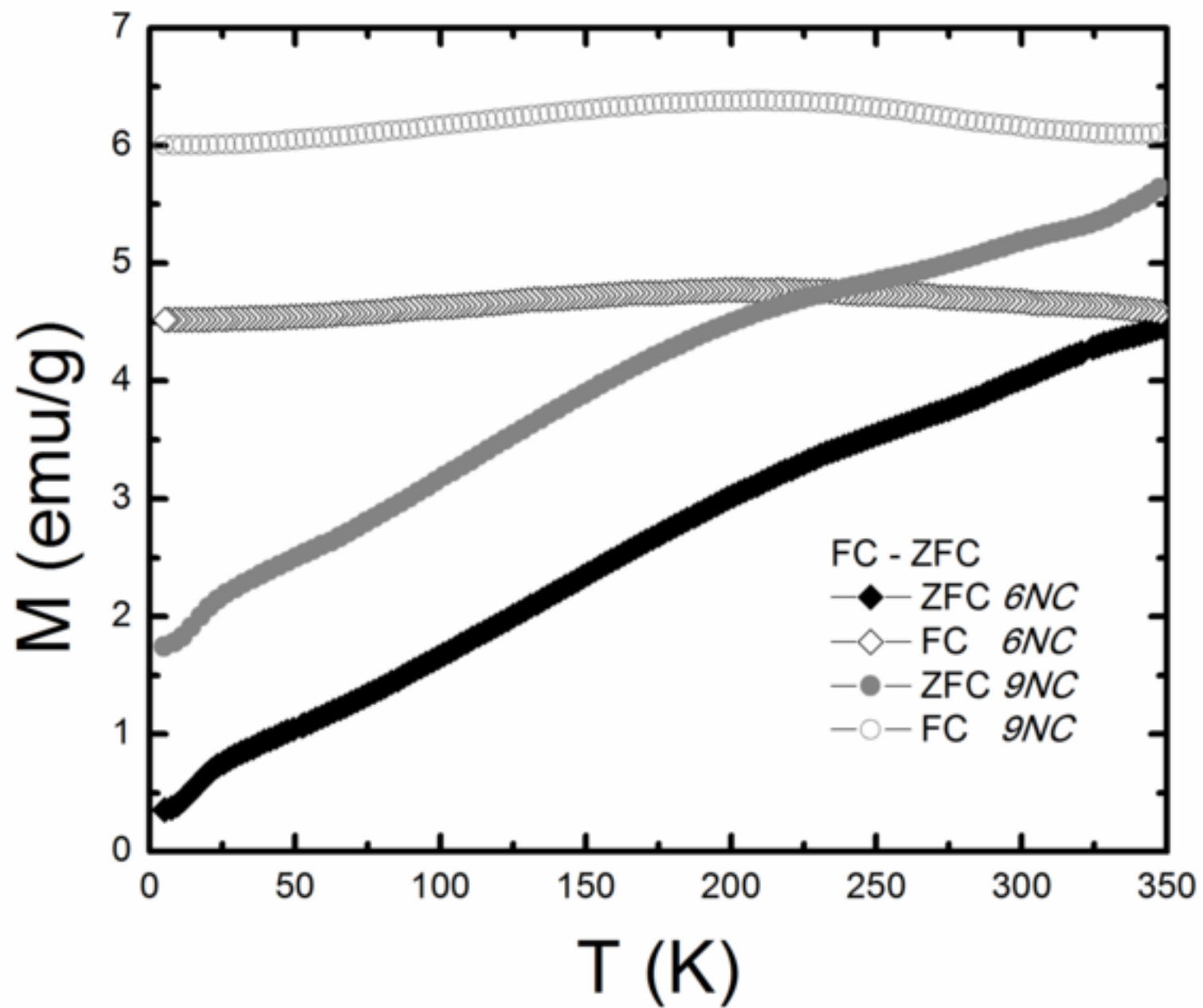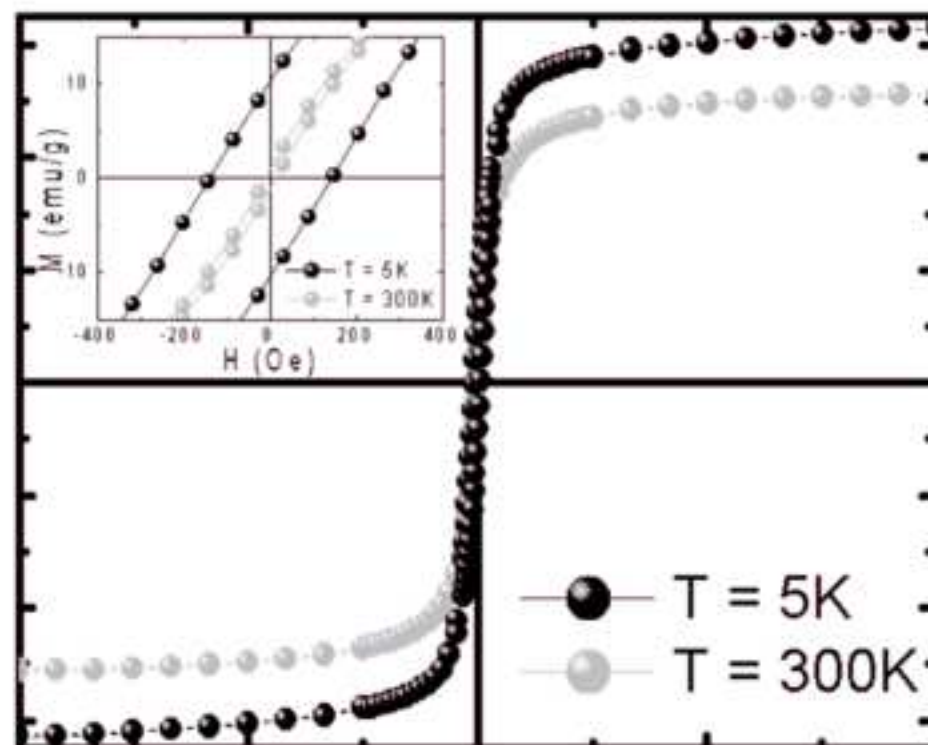
Highlights: > Ferrogels were obtained by freezing thawing of PVA/PAA-coated magnetic NPs > Strong H-bonding between PAA-PVA allowed homogeneous dispersion of NPs in the matrix> Polyelectrolyte nature of the coating increased swelling of the ferrogels > Magnetic and physical properties make these gels promising for biomedical applications.